Published OnlineFirst February 25, 2011; DOI: 10.1158/1541-7786.MCR-10-0358

Molecular Cancer Research

Activation of Interferon-Stimulated Genes by γ-Ray Irradiation Independently of the Ataxia Telangiectasia Mutated–p53 Pathway

Takashi Sugihara[1], Hayato Murano[2], Masako Nakamura[2], Kazuaki Ichinohe[1], and Kimio Tanaka[1]

Abstract

The ataxia telangiectasia mutated (ATM)-p53 pathway is a well-known main signal transduction pathway for cellular responses, which is activated by γ-ray irradiation. Microarray analysis showed changes in the expressions of IFN-stimulated genes (ISG) in γ-ray–irradiated Balb/cA/*Atm*-deficient mouse embryonic fibroblasts (MEF) (ATM-KO), indicating that another pathway for cellular responses besides the ATM-p53 pathway was activated by γ-ray irradiation. The basal expression levels of *Irf7* and *Stat1* in ATM-KO and *p53*-deficient MEFs (p53-KO) were higher than those in *Atm*–wild-type MEFs (ATM-WT) and *p53*-wild-type MEFs (p53-WT), respectively. Irradiation stimulated the expressions of *Irf7* and *Stat1* in ATM-KO, p53-KO, ATM-WT, and p53-WT, indicating that upregulation of *Irf7* and *Stat1* expressions by irradiation did not depend on the ATM-p53 pathway. When conditioned medium (CM) obtained from irradiated ATM-WT or ATM-KO was added to nonirradiated MEFs, the expressions of *Irf7* and *Stat1* increased. We predicted that gene activation in nonirradiated MEFs was caused by IFN-α/β. Unexpectedly, significant amount of IFN-α/β could not be detected in the CM from irradiated ATM-WT or ATM-KO. Meanwhile, increased expression of Ccl5 (RANTES) protein was detected in the CM from irradiated MEFs. These results indicate that ISGs were activated by γ-ray irradiation independently of the ATM-p53 pathway and gene activation was caused by radiation-induced soluble factors. *Mol Cancer Res; 9(4); 476–84. ©2011 AACR.*

Introduction

Cell signaling pathways such as the ataxia telangiectasia mutated (ATM)-p53 pathway activated by γ-ray irradiation have been well studied. Irradiated cells are known to accumulate p53 immediately after radiation-induced DNA damage, resulting in the induction of cell cycle arrest at the G1 phase or apoptosis (1). Phosphoinositide 3-kinases such as ATM and DNA-dependent protein kinase, catalytic subunit (DNA-PKcs) are activated after radiation-induced DNA double-strand breaks. ATM phosphorylates p53 at Ser15/18, leading to its stabilization through the inhibition of murine double minute 2-dependent degradation (2). Many proteins associated with cell cycle checkpoint control, apoptotic responses, and DNA repair, for example, p53, Chk2, and others, are phosphorylated by ATM (3, 4). Therefore, DNA damage-dependent pathway such as that associated with ATM-p53 or DNA-PKcs has been the major focus in radiation biology. Recently, another pathway besides the ATM-p53 pathway has been reported. Sphingomyelinase is activated by irradiation independently of the ATM-p53 pathway to produce ceramide, which in turn, can induce signals of c-Raf and downstream genes of the mitogen-activated protein kinase superfamily members (5, 6). Furthermore, ATM-knockdown HeLa cells produced by treating with *Atm*-targeting siRNA showed 10-fold upregulation of IFN-stimulated genes (ISGs) after irradiation (7). Hence, we focused on the radiation-induced pathway that was independent of ATM-p53. To clarify the activation of this pathway by γ-ray irradiation, gene expressions in *Atm*-deficient mouse embryonic fibroblasts (MEF; ATM-KO) and *Atm*-wild-type MEFs (ATM-WT) were compared by microarray analysis.

Radiation-induced bystander effects are well-known phenomena, in which genomic aberration(s) or altered cellular responses in nonirradiated cells are induced by irradiated neighbor cells. However, the underlying molecular mechanism has not been sufficiently elucidated. Mothersill and Seymour originally found another type of radiation-induced bystander effect, in which nonirradiated cells showed a decreased ability of colony formation after treatment with conditioned medium (CM) obtained from irradiated cells

Authors' Affiliations: [1]Department of Radiobiology, Institute for Environmental Sciences, Takahoko, Rokkasho, Kamikita; and [2]Tohoku Environmental Sciences Services Corporation, Mutsu, Aomori, Japan

Note: Supplementary data for this article are available at Molecular Cancer Research Online (http://mcr.aacrjournals.org/).

Corresponding Author: Takashi Sugihara, Department of Radiobiology, Institute for Environmental Sciences, 2-121 Hacchazawa, Takahoko, Rokkasho, Kamikita, Aomori 039-3213, Japan. Phone: 175-71-1746; Fax: 175-71-1982. E-mail: sugihara@ies.or.jp

doi: 10.1158/1541-7786.MCR-10-0358

Published OnlineFirst February 25, 2011; DOI: 10.1158/1541-7786.MCR-10-0358

(8). Several recent papers have indicated that p53 accumulation in irradiated cells can attenuate the secretion of nitric oxide synthase through the interaction of p53 with both TATA-binding protein and NF-κB (9, 10). Furthermore, Yang and colleagues reported that CM-mediated intercellular communication caused bystander effects through toxic factors, other than reactive oxygen species, released from irradiated cells into the CM of cultured cells (11). However, studies identifying the soluble factors associated with the induction of bystander effects are quite few. In this study, microarray analysis showed that the expressions of several ISGs were upregulated in irradiated ATM-KO. Thus, we speculated that the CM from irradiated ATM-KO had high activity for ISG expression. To clarify this activity of the CM from irradiated ATM-KO for ISG expression, the collected CM was analyzed using a cell-based assay for ISG expression, and cytokine expression in the CM from irradiated ATM-KO was measured. We focused on 2 points in this study: one was to identify a new ATM-independent signaling pathway activated by irradiation, and the other was to identify a possible recurrent radiation-induced bystander effect mediated by CM.

Materials and Methods

Establishment and culture of MEFs

Atm heterozygous mice derived from *Atm*-targeted mice (129/SvEv-*Atm*$^{tm1Awb/+}$) were kindly supplied by the Radiation Biology Center, Kyoto University, courtesy of Dr. O. Niwa. The sequence of the *Atm* gene was analyzed by previously described genomic PCR method (12). *Atm*$^{+/+}$: ATM-WT and *Atm*-deficient MEFs (*Atm*$^{-/-}$: ATM-KO) were established from 12- to 14-day-old embryos produced by crossing Balb/cHeA/*Atm*$^{+/-}$ mice. *p53*-wild-type MEFs (p53-WT) and *p53*-deficient MEFs (p53-KO) were established from 12- to 14-day-old embryos produced by crossing *p53*-hetero C3H mice [C3H/HeN-TgH(*p53*); Accession no. CDB0001K] obtained from RIKEN BioResource Center, and the sequence of the *p53* gene was analyzed by previously described genomic PCR method (13). In addition, MEFs were established from C.B-17/Icr$^{+/+}$Jcl mice (CLEA Japan Inc.). The established MEFs were maintained for 3 to 6 passages and used for irradiation experiments and gene and protein analyses. Balb/cA/ATM-WT, Balb/cA/ATM-KO, C3H/*p53*-wild-type MEFs, C3H/*p53*-knockout MEFs, and C.B-17/Icr MEFs are indicated as ATM-WT, ATM-KO, p53-WT, p53-KO, and ICR-MEFs, respectively, in this article.

^{137}Cs γ-ray irradiation

A suspension of each type of MEFs (8 mL; 5×10^4–10×10^4 cells/mL) in Advanced Dulbecco's modified Eagle's medium (DMEM) containing 10% FBS was added to culture flask, and incubated for 1 day at 37°C in a CO_2 incubator. ^{137}Cs γ-ray irradiation at a dose rate of 0.9 Gy/min for a total dose of 4.32 Gy was conducted using Gammacell 40 (MDS Nordion). The irradiated and nonirradiated MEFs were cultured and harvested at 1 to 3 days after irradiation, and their total RNAs were dissolved in 500 μL Trizol (Invitrogen) for extraction and subsequent analysis.

Culture of MEFs in the presence of ATM inhibitor

An ATM-specific inhibitor (KU55933; Sigma-Aldrich; ref. 14) was dissolved in dimethyl sulfoxide (DMSO) at final concentrations of 0.16, 0.4, 2, and 10 μmol/L. As a control, 0.1% DMSO alone was used. According to a standard protocol, KU55933 was added to the CM 1 hour before irradiation. ATM-WT was cultured in the medium containing KU55933 for 3 days at 37°C in a 5% CO_2 incubator.

Gene expression analysis by microarray

Irradiated and nonirradiated ATM-WT and ATM-KO were harvested at 3 days after irradiation. After RNA extraction from the harvested cells, gene expression was analyzed by microarray analysis (whole mouse genome oligo DNA microarray; Agilent). RNA samples were labeled with Cy3 (Agilent) and hybridized to the oligo microarray chips at 65°C for 17 hours. After washing and drying, each array was scanned using Agilent DNA Microarray Scanner, and the images were processed using Agilent Scan Control software. The "Gene Ontology" (GO) function in GeneSpring GX 11 software (Agilent) was used for the classification and measurement of whole-gene expression levels. Signal transduction pathways were analyzed with the Ingenuity Pathway Analysis (IPA) software (Ingenuity Systems).

Gene expression analysis by real-time PCR

The expression levels of several genes such as *Irf7* and *Stat1*, detected to be significantly high or low by microarray analysis, were confirmed by conducting quantitative real-time PCR (ABI. 7700; Applied Biosystems) to measure the levels of mRNA expression in the MEFs. The methods of total RNA isolation and reverse transcriptase (RT)-mix preparation were as described previously (15, 16). The cDNAs of glyceraldehyde-3-phosphate dehydrogenase gene (*Gapdh*) were amplified and quantified as a control for RNA expression. The sense and antisense oligonucleotides used as primers and TaqMan probes for the detection of *Irf7* and *Stat1* were as follows: *Irf7*-TaqManProbe, 5′-ACC CCG TCC CAC CAC AGG CTC C-3′; *Irf7*-Forward, 5′-CAC ATA CTG GAA TCC GAG TCT GG-3′; *Irf7*-Reverse, 5′-GCC ATG CTG CAT AGG GTT CC-3′; *Stat1*-Forward (Syber probe), 5′-ACA ACA TGC TGG TGA CAG AGC C-3′; *Stat1*-Reverse, 5′-TGA AAA CTG CCA ACT CAA CAC CTC-3′. The primers used for the detection of *Gapdh* were as described previously (15, 16).

Protein expression analysis by Western blotting

The expression levels of Irf7, Stat1, phosphorylated Stat1 (p-Stat1-Ser727), p53, and phosphorylated p53 (p-p53-Ser15/18) were analyzed by Western blotting. Proteins extracted from the irradiated and nonirradiated MEFs were dissolved in SDS sample buffer. β-Actin antibody (AC-15; Abcam) was used as a quantity control for protein expression.

Published OnlineFirst February 25, 2011; DOI: 10.1158/1541-7786.MCR-10-0358

Anti–phospho-p53 (Ser15/18; Cell Signaling Technology), anti-Irf7 (Invitrogen), anti-Stat1 (Cell Signaling Technology), and anti–phospho-Stat1 (Ser727; Cell Signaling Technology) were used as primary antibodies for the analysis of protein expression.

Analysis of *Irf7* and *Stat1* expression in nonirradiated MEFs after addition of CM collected from irradiated MEFs

CM was obtained from ATM-WT or ATM-KO at 3 days after irradiation at 0.9 Gy/min for a total dose of 4.32 Gy. To evaluate the CM activity for the expression of each gene, ICR-MEFs were used in a cell-based assay; they were cultured without irradiation for 1 day after addition of each collected CM (1 mL). The expressions of *Irf7* and *Stat1* were analyzed by real-time PCR methods after addition of the CM. To confirm the effect of regulated on activation by secreted [regulated upon activation, normal T cell expressed and secreted (RANTES); Ccl5] or 10-kDa IFN-γ–inducible protein (IP-10; Cxcl10) on gene expressions, fresh DMEM with 10% FBS and various concentrations of either human recombinant RANTES (hrRANTES; Acris Antibodies GmbH) or human recombinant IP-10 (hrIP-10; Affinity BioReagents Inc.) were added to the ICR-MEFs in the cell-based assay.

Protein expression analysis in CM by cytokine ELISA

The expressions of IFN-α/β, IFN-γ, Ccl5 (RANTES), and Ccl3 [macrophage inflammatory protein 1α (Mip-1α)] in the CM from ATM-WT and ATM-KO were measured using IFN-α/β ELISA kit (PBL InterferonSource), IFN-γ ELISA kit (BD), mouse RANTES Instant ELISA kit (Bender MedSystems), and mouse Mip-1α Immunoassay kit (R&D Systems Inc.), respectively.

Results

Microarray analysis of gene expression in ATM-KO

The expression patterns of whole mRNAs were analyzed by microarray to elucidate the change in signal transduction in ATM-KO after γ-ray irradiation. We previously showed that changes at 3 days after irradiation were different from those in the early phase of irradiation (4 hours); thus, we selected the changes in the late phase (3 days) for microarray analysis (15, 16). A total of 30,093 genes were confirmed by 2-way ANOVA to be of superior quality for use in the microarray analysis. The total number of genes with significantly ($P < 0.05$) low or high expression in ATM-KO, which showed loss of ATM function, was 203. These genes were classified into 2 clusters: cluster A consisted of 124 genes and cluster B consisted of 79 genes (Fig. 1A, left). Cluster A mainly consisted of the genes downregulated because of loss of ATM function. Furthermore, 95 GO accessions were significantly ($P < 0.01$) detected in cluster A by a computational GO search (Supplementary Table S1). The total number of genes with significantly ($P < 0.05$) increased or decreased expression in ATM-KO after irradiation was 276. These genes were classified into 2 clusters: cluster C consisted of 144 genes and cluster D consisted of 132 genes (Fig. 1A, right). Cluster C mainly consisted of the genes downregulated by irradiation. Furthermore, 24 GO accessions were significantly ($P < 0.01$) detected in cluster C (Supplementary Table S1). Genes in both clusters B and D were coordinately upregulated by loss of ATM function and irradiation, and only 34 genes were detected in both clusters B and D, which were upregulated by combined effects of loss of ATM function and irradiation. Three GO accessions were detected only in cluster B, and 3 other GO accessions were detected only in cluster D (Supplementary Table S1). Notably, 5 GO accessions, involving "immune response," "immune system process," "response to virus," and others, were detected in both clusters B and D (Supplementary Table S1).

IPA of genes in clusters A and B could detect a pathway involving chemokine genes such as *Ccl3l3*, *Ccl4*, and *Ccl5* (Fig. 1B). The ratios (nonirradiated ATM-KO/nonirradiated ATM-WT) of the expression levels of genes such as *Ccl2*, *Ccl3l3*, and *Ccl4*, which are activated by fibrinogen (17, 18), were much decreased in nonirradiated condition (Fig. 1B). On the other hand, the ratios of the expression levels of ISGs such as *Stat1*, *Irf7*, and *Oas3* were increased without irradiation, by the loss of ATM function (Fig. 1B). Furthermore, IPA of genes in clusters C and D could detect a pathway involving several ISGs such as *Irf7* and *Stat1* and chemokines genes such as *Ccl5* (Fig. 1C). The ratios (irradiated condition/nonirradiated condition) of the expression levels of these genes were much increased in both ATM-KO and ATM-WT after irradiation. These results indicate that upregulation of the expressions of ISGs was induced by either loss of ATM function or irradiation.

Expression of *Irf7* and *Stat1* and corresponding proteins in irradiated ATM-KO

Both *Irf7* and *Stat1* are well-known ISGs, whose products play an important role in IFN production and signal transduction in response to viral infection (19, 20). Because *Irf7* and *Stat1* were detected by IPA (Fig. 1B, 1C), they were also implicated to play important roles in radiation response under conditions of ATM deficiency. Therefore, we focused on *Irf7* and *Stat1* to elucidate the expressions of ISGs after irradiation. The expression levels of these 2 genes were quantitatively analyzed by real-time PCR at 1, 2, and 3 days after γ-ray irradiation (total dose, 4.32 Gy). The expressions of *Irf7* and *Stat1* at 3 days were significantly higher than those at 1 day. Furthermore, the expressions in nonirradiated ATM-WT at 3 days increased little, but those in irradiated ATM-WT much increased from 2 days (Fig. 2A). On the other hand, the expressions in both nonirradiated and irradiated ATM-KO were remarkably increased from 2 days (Fig. 2A). The expressions in nonirradiated ATM-KO were significantly ($P < 0.05$) higher than those in nonirradiated ATM-WT (Fig. 2A). This result indicates that ATM deficiency caused an increase in the basal expression levels of *Irf7* and *Stat1*. Furthermore, those expressions at 3 days in irradiated ATM-WT and ATM-KO were significantly ($P < 0.05$) higher than those in nonirradiated

Published OnlineFirst February 25, 2011; DOI: 10.1158/1541-7786.MCR-10-0358

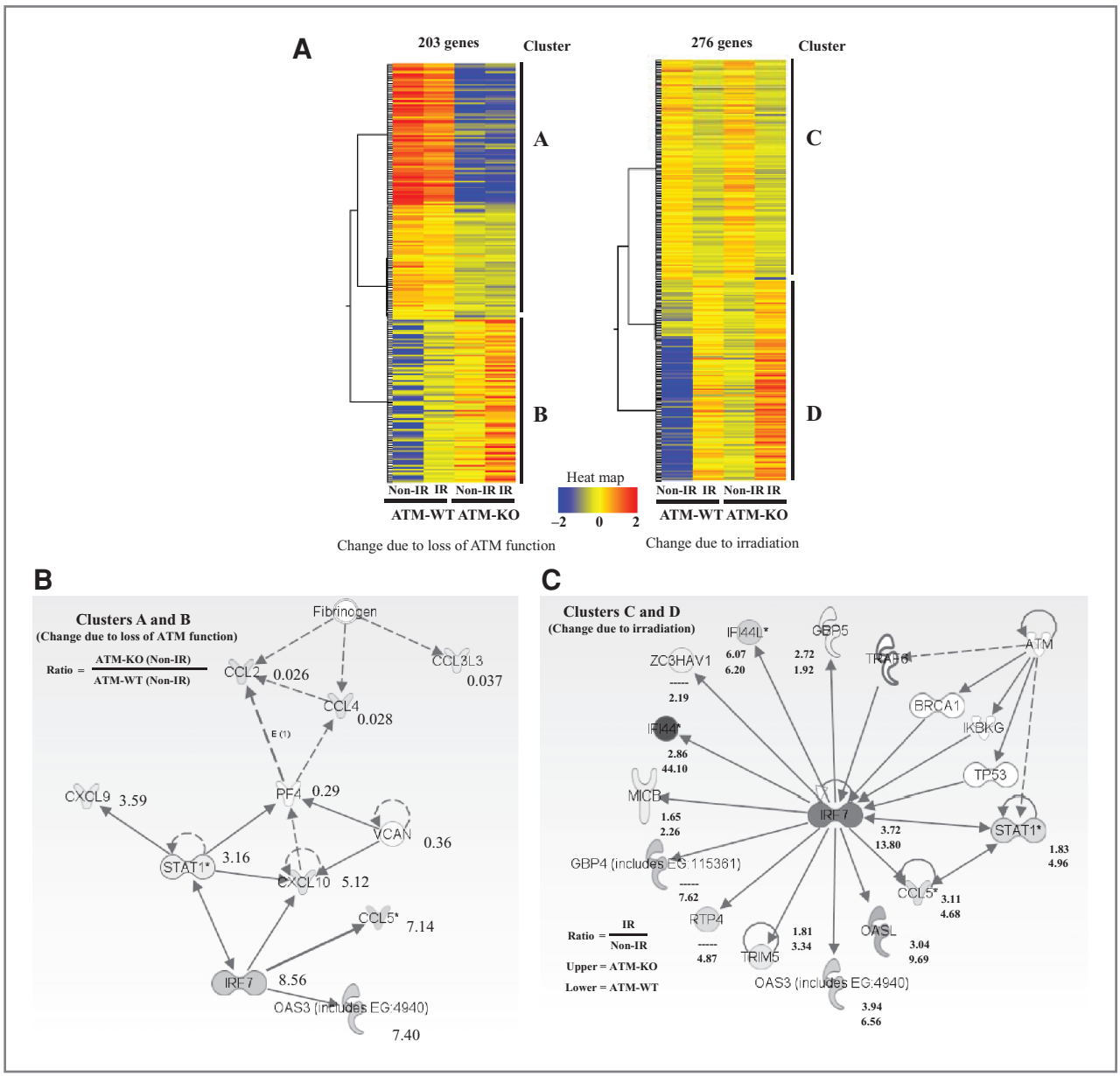

Figure 1. A, clustering of genes into 4 different groups (clusters A, B, C, and D), according to their expressions in ATM-WT and ATM-KO with irradiation (IR) and without irradiation (non-IR). Three independent experiments were done and the data obtained were summarized. Significantly ($P < 0.05$) high and low expression levels of genes were detected in each condition and analyzed by 2-way ANOVA and a multiple testing correction (Benjamini–Hochberg false discovery rate). The 4 clusters were identified using "2 × 2 self-organized cluster analysis" in GeneSpring GX 11. The heat map shows a graded color coding for the expression level of each gene, in which red and blue indicate upregulated and downregulated genes, respectively. Furthermore, each cluster was analyzed by conducting a GO search, and the GO terms detected in each of the 4 clusters are listed (Supplementary Table S1). B, pathway extracted for clusters A and B, whose genes were expressed as a result of loss of ATM function, using GeneSpring GX 11 and IPA. Symbols indicate gene name which were obtained from previous studies. Lines connecting 2 genes show the relationship between the genes, with the continuous and broken arrows indicating "upregulation" and "downregulation," respectively. The number beside a gene (gene symbol), which indicates gene expression, show fold change in the gene expression levels (ATM-KO non-IR/ATM-WT non-IR). C, pathway extracted for clusters C and D, whose genes were expressed as a result of irradiation. The upper number beside each gene, which indicates upregulated expression, shows fold change in the gene expression levels in ATM-KO; IR ATM-KO/non-IR ATM-KO. The lower number beside each gene, which indicates downregulated expression, shows fold change in the gene expression levels in ATM-WT (IR ATM-WT/non-IR ATM-WT). Gray symbol for a gene indicates upregulated expression, and white symbol for a gene indicates less than 1.5-fold change in expression.

ATM-WT and ATM-KO, respectively (Fig. 2B), which indicates that radiation could induce the expressions of *Irf7* and *Stat1* without ATM. Moreover, the expressions of p-p53-Ser15/18, Irf7, Stat1, and p-Stat1-Ser727 in irradiated ATM-WT and ATM-KO were higher than those in nonirradiated ATM-WT and ATM-KO, respectively

Published OnlineFirst February 25, 2011; DOI: 10.1158/1541-7786.MCR-10-0358

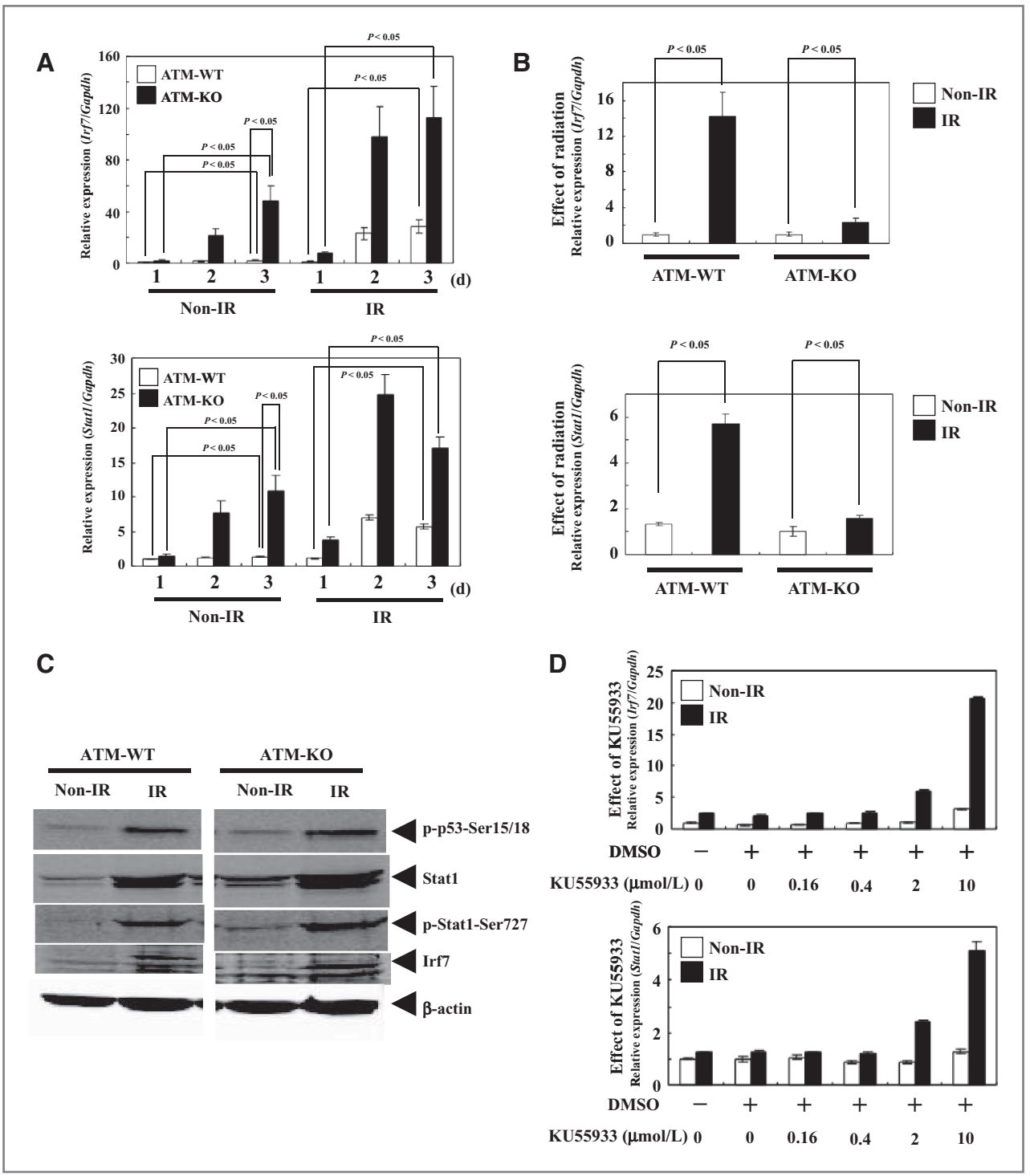

Figure 2. A, the expression levels of *Irf7* and *Stat1* in ATM-WT and ATM-KO; (non-IR, nonirradiated; IR, irradiated) at 1, 2, and 3 days after irradiation were quantitatively analyzed by real-time PCR. *Gapdh* was used as an internal control, and statistical significance was determined by *t* test. B, the expression levels of *Irf7* and *Stat1* in ATM-WT and ATM-KO at 3 days after IR were quantitatively analyzed by real-time PCR, and radiation effects in each type of MEFs were estimated by comparing the expression levels with those in the same type of non-IR MEFs. *Gapdh* was used as an internal control, and statistical significance was determined by *t* test. C, the expression levels of Irf7, Stat1, p-p53-Ser15/18, and p-Stat1-Ser727 in ATM-WT and ATM-KO; (Non-IR, nonirradiated; IR, irradiated) at 3 days after irradiation were compared with Western blotting. β-Actin was used as an internal control. D, the expression levels of *Irf7* and *Stat1* in ATM-WT treated with KU55933 (0, 0.16, 0.4, 2, and 10 μmol/L), at 3 days after irradiation (IR), were quantitatively analyzed by real-time PCR, and the basal expression levels were estimated by comparing with the ratios in nonirradiated (Non-IR) ATM-WT cultured without DMSO and KU55933. *Gapdh* was used as an internal control, and statistical significance was determined by *t* test.

Published OnlineFirst February 25, 2011; DOI: 10.1158/1541-7786.MCR-10-0358

(Fig. 2C). To analyze the expressions of *Irf7* and *Stat1* under the condition of inhibited ATM kinase activity, the gene expressions in ATM-specific inhibitor (KU55933)-treated ATM-WT–which are mimics of ATM-KO–were compared with those in ATM-WT cultured with 0.1% DMSO alone as a control. The gene expressions were upregulated by irradiation, but 0.1% DMSO played no role in the radiation-induced upregulation of the gene expressions. Furthermore, 2 μmol/L and 10 μmol/L of KU55933 enhanced the gene expressions in irradiated ATM-WT (Fig. 2D), which indicates that radiation could induce the expressions of *Irf7* and *Stat1* and that the ATM-specific inhibitor KU55933 could also enhance the gene expressions in irradiated ATM-WT.

Expression of *Irf7* and *Stat1* in irradiated p53-KO

The ATM-p53 pathway is a well-known main signal transduction pathway for cellular responses, which is activated by γ-ray irradiation. Therefore, we focused on the p53 signaling pathway after irradiation of p53-KO. The basal expression levels of *Irf7* and *Stat1* in p53-KO were higher than those in p53-WT (Fig. 3), which is a similar tendency as that seen in the comparison of ATM-KO and ATM-WT (Fig. 2B). Furthermore, the gene expressions in irradiated p53-WT and p53-KO were slightly increased (Fig. 3), and treatment with the ATM-specific inhibitor KU55933 slightly enhanced the expressions of the genes (Fig. 3) in both irradiated p53-WT and p53-KO. These results indicate that *p53* deficiency caused an increase in the basal expression levels of *Irf7* and *Stat1* and that the gene expressions were enhanced by irradiation independently of p53.

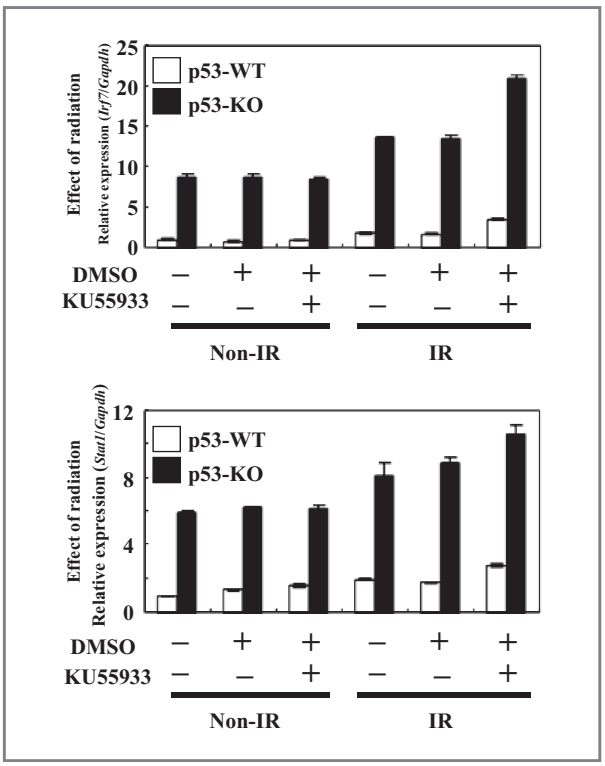

Figure 3. The expression levels of *Irf7* and *Stat1* in p53-WT and p53-KO treated with KU55933 (10 μmol/L), at 3 days after irradiation (IR), were quantitatively analyzed by real-time PCR, and the basal expression levels in each type of MEFs were estimated by comparing with the ratios in the same type of nonirradiated (Non-IR) MEFs cultured without DMSO and KU55933. *Gapdh* was used as an internal control, and statistical significance was determined by *t* test.

Expression of cytokines in CM from irradiated MEFs

CM collected from irradiated ATM-WT or ATM-KO was assayed using a cell-based assay, which was done to measure the CM activity for the expressions of *Irf7* and *Stat1* in ICR-MEFs. ICR-MEFs were used as standard cells because we confirmed that they had high sensitivity for the expressions of *Irf7* and *Stat1* by irradiation or treatment with ATM inhibitor in preliminary experiments. The CM collected from nonirradiated ATM-WT at 1 to 3 days showed no activity for the expressions of *Irf7* and *Stat1*, whereas that collected from irradiated ATM-WT at 2 to 3 days showed slightly increased activity (Fig. 4A). On the other hand, the CM collected from both nonirradiated and irradiated ATM-KO at 2 to 3 days showed much increased activity for the gene expressions (Fig. 4A). These results indicate that the CM-mediated expressions of *Irf7* and *Stat1* depend on irradiated or *Atm*-deficient condition. Thus, we predicted that the factor responsible for ISG activation was IFN-β in the CM, because upregulated expression of *Ifnb1* was observed in the microarray analysis conducted in this study. The amount of IFN-α/β/γ in the CM collected from irradiated or nonirradiated MEFs was then measured by ELISA; however, a significant detectable level of IFN-α/β/γ was not observed in the CM from both irradiated ATM-WT and ATM-KO (data not shown). From these results, we predicted that the enhanced expressions of *Irf7* and *Stat1* in the CM from γ-ray–irradiated ATM-WT or ATM-KO might be induced by cytokines other than IFN-α/β/γ in the CM.

Two cytokine genes appearing in the IPA maps, *Ccl5* (RANTES) and *Ccl3l3* (Mip-1α) (Fig. 1B, 1C), were selected for further analysis. Their encoded proteins were quantified by ELISA to determine their presence in the CM from irradiated ATM-WT or ATM-KO. The amount of RANTES (Ccl5) in the CM collected from irradiated ATM-KO at 1 to 3 days was higher than that in the CM collected from irradiated ATM-WT (Fig. 4B). Furthermore, the amount of RANTES (Ccl5) in the CM collected from irradiated ATM-WT at 2 to 3 days was higher than that in the CM collected from nonirradiated ATM-WT (Fig. 4B). These results indicate that the production of RANTES in the CM collected from irradiated MEFs might be related to the enhanced expressions of *Irf7* and *Stat1*. On the other hand, no increase was observed in the amount of Ccl3l3 (Mip-1α) in the CM collected from either irradiated or nonirradiated ATM-KO at 1 to 3 days after irradiation (Fig. 4B). These ELISA results were consistent with the

Published OnlineFirst February 25, 2011; DOI: 10.1158/1541-7786.MCR-10-0358

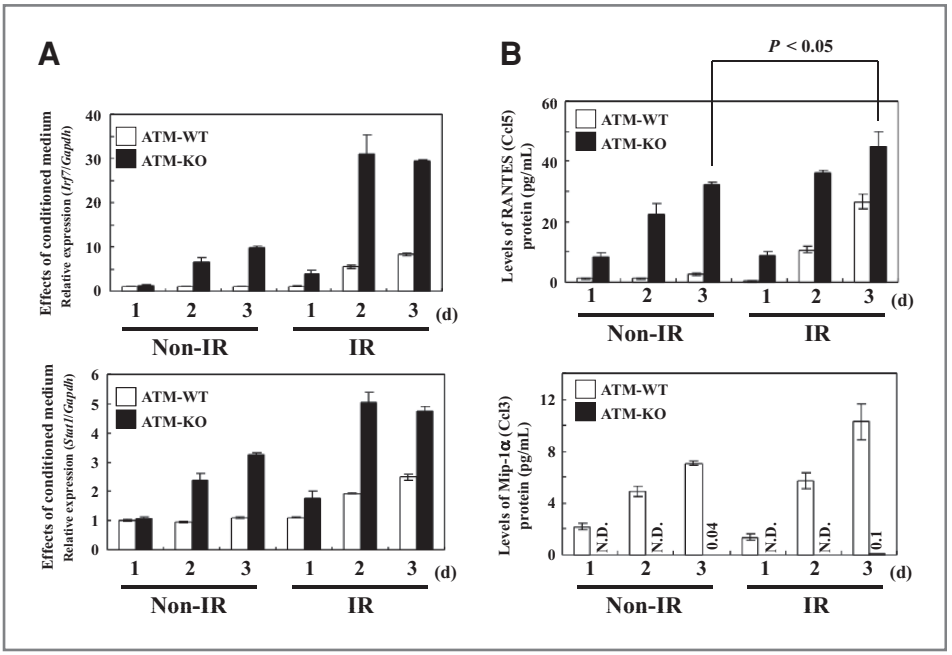

Figure 4. A, cell-based assay for the expressions of *Irf7* and *Stat1* determined by real-time PCR at 1 to 3 days after irradiation. CM collected from ATM-WT and ATM-KO cultured for 1 to 3 days under irradiated (IR) or nonirradiated (Non-IR) condition was added to nonirradiated ICR-MEFs, following which the ICR-MEFs were cultured for 1 day. Thereafter, the expression levels of *Irf7* and *Stat1* in the nonirradiated ICR-MEFs were analyzed. *Gapdh* was used as an internal control, and statistical significance was calculated by *t* test. B, secreted protein levels of RANTES (Ccl5) and Mip-1α Ccl3 levels in the CM collected from ATM-WT and ATM-KO cultured for 1 to 3 days under IR or Non-IR condition were measured by ELISA. N.D., not detectable levels. and values shown in graph indicate levels of Mip-1α. Statistical significance was determined by *t* test.

microarray analysis results. Furthermore, to observe the function of chemokines such as Ccl5 (RANTES) and Cxcl10 (IP-10)–which were detected by IPA (Fig. 1B)–in the CM, purchased hrRANTES and hrIP-10 (0–1000 pg/mL) were added to the CM, respectively, for analyzing the activity for the expressions of *Irf7* and *Stat1*. However, the gene expressions were not significantly enhanced by the addition of any concentration of hrRANTES and hrIP-10 in the CM (data not shown). These results indicate that the increased amounts of Ccl5 (RANTES) and Cxcl10 (IP-10) in the CM from irradiated MEFs had no effect on the induction of the expressions of *Irf7* and *Stat1* and that unknown soluble factors in the CM from irradiated ATM-WT or ATM-KO might have upregulated the expressions of the 2 genes.

Discussion

Atm-knockdown HeLa cells, produced using *Atm*-targeting siRNA, showed induction of the expressions of ISGs by irradiation, although the biological significance of this finding has not been clarified (7). Also, upregulation of ISGs was observed in γ-ray–irradiated *Atm*-deficient MEFs in this study. These results indicate that upregulation of ISGs by γ-ray irradiation was not related to the ATM-p53 signal transduction pathway. Furthermore, we predicted that the soluble factor responsible for ISG activation in the CM from irradiated MEFs might be IFN-α/β/γ. IFN-α/β expression is known to be stimulated by immune responses during viral infections, such as through the Toll-like receptor (TLR) pathway; TLR triggers the induction of type I IFN (IFN-α/β), providing a crucial mechanism of antiviral defense. Moreover, Irf7 is known to be a master regulator of type I IFN-dependent immune responses (21). Thus, IFN-α/β expression is stimulated by Irf7, and Irf7 induces ISG expression through a positive feedback loop (19). The positive feedback during viral infection is illustrated in the top panel of Figure 5. Unexpectedly, the amount of IFN-α/β/γ in the CM from irradiated Balb/cA MEFs (ATM-WT and ATM-KO) could not be detected in significant levels by ELISA in this study, and it was considered that radiation-induced activation of *Irf7* and *Stat1* might be caused by unknown soluble factors. Otherwise, the gene expressions might be stimulated by undetectable levels of IFN-α/β/γ because the cell-based assay could detect high CM activity for the gene expressions. The activity for *Irf7* and *Stat1* expression after the addition of the CM from nonirradiated ATM-KO was higher than that after the addition of the CM from nonirradiated ATM-WT. Thus, *Atm* deficiency itself may produce unknown soluble factors for the upregulation of the expressions of *Irf7* and *Stat1* without irradiation. Hence, we concluded that viral stimulation and irradiation may use quite different pathways for the stimulation of *Irf7* and *Stat1* expression (Fig. 5).

Basal expression levels of ISGs in nonirradiated *Atm*- or *p53*-deficient MEFs were higher than those in each nonirradiated wild-type MEFs, which indicate that nonphosphorylated ATM or p53 without γ-ray radiation-induced DNA double-strand breaks may be suppressing ISGs activation. Townsend and colleagues have also reported enhanced Stat1 expression in p53-KO (22). It is well known that radiation-induced ATM activation leads to the accumulation of p53. This study experiments also showed that treatment with ATM inhibitor enhanced the expressions of *Irf7* and *Stat1* in irradiated p53-KO, which indicated that the radiation-induced increase in ISG expression was not related to the activation of the ATM-p53 pathway. Takaoka and colleagues have shown

Published OnlineFirst February 25, 2011; DOI: 10.1158/1541-7786.MCR-10-0358

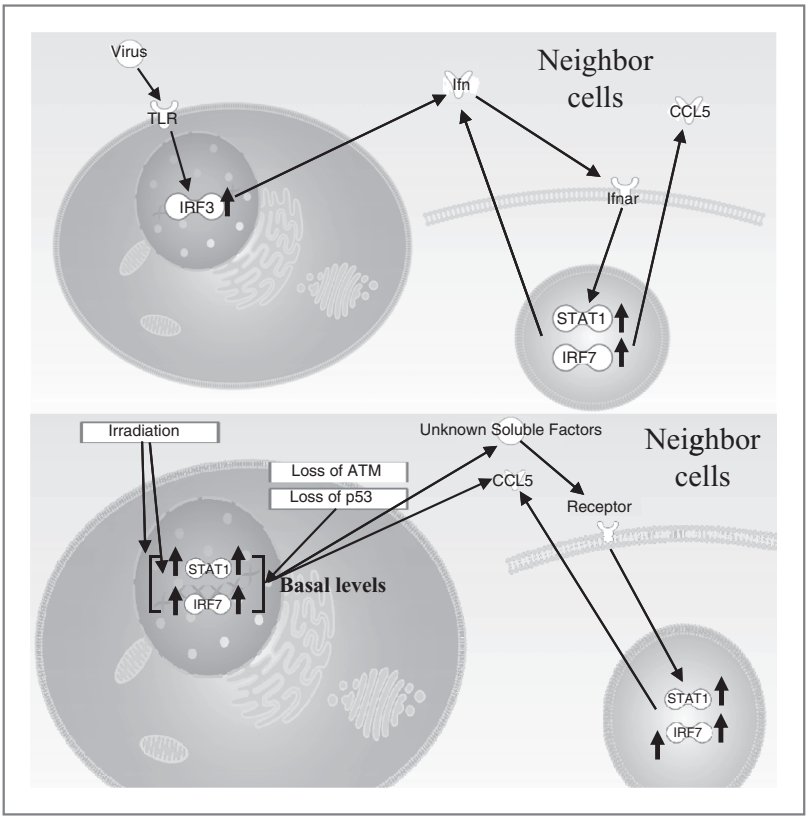

Figure 5. Model for presumed signal transductions on γ-ray irradiation. Neighbor cells are influenced by radiation-induced soluble factors. IRF, interferon regulatory factor; IFN-αR, IFN-α receptor; CCL5; CC chemokine ligand 5; STAT1signal transducer and activator of transcription 1.

that *p53* activation is induced by viral infection, through IFN-α/β production (23); thus, *p53* is considered to be downstream of ISGs. Moreover, it has been reported that *Stat1*-deficient cells show reduced Chk2-Thr68 phosphorylation on irradiation, and Stat1 is required for ATM-dependent phosphorylation of Nijmegen breakage syndrome 1 (NBS1) and p53 following DNA damage (22). Thus, radiation-induced expression of *Stat1* in ATM-WT, as observed in this study, may activate phosphorylation of Chk2, NBS1, and p53. Other kinases such as ataxia telangiectasia and Rad3-related (ATR) or DNA-PKcs, which have both been shown to phosporylate ATM substrates, might be replaced ATM in the absence of ATM. Our preliminary experiments, *Irf7* and *Stat1* in Scid-MEFs derived from Scid-mice which have known to *DNA-PKcs*-deficient mice, and ICR-MEFs which have known to wild-type mice for Scid-mice, respectively, were also upregulated by irradiation, but basal levels of their genes expressions in Scid-MEFs were not upregulated to compare with ICR-MEFs (data not shown). Thus DNA-PKcs did not relate with basal expression levels of *Irf7* and *Stat1* and upregulations of their gene expressions by γ-ray irradiation. Furthermore, ATR-deficient MEFs were not done in present experiments, so ATR may be relate with gene expressions of *Irf7* and *Stat1* in the absence of ATM, but we do not conclude ATR-role in present studies.

Radiation-induced bystander effects are considered to be induced indirectly by cytokines or nitric oxides (9, 10, 11). Significantly high expressions of *Ccl5* and *Cxcl10*, which encode chemotactic chemokines involved in cell migration, were detected in irradiated or *Atm*-deficient condition in the microarray analysis conducted in this study (Figs. 1C and 4B). *Ccl5* (RANTES) promoter is stimulated by Irf7, and upregulation of IFN-inducible chemokines (*Ccl5*, *Cxcl9*, and *Cxcl10*) is always observed in tumor-associated macrophages activated by lipopolysaccharides (24). Thus, the expression of *Ccl5* (RANTES) in irradiated MEFs might be induced by radiation-induced Irf7. Monocyte/macrophage and lymphocyte recruitment and activation are the key components of the mechanism of radiation-induced fibrosis through CC chemokine ligand (CC) and CXC chemokine ligand (CXC) family members such as Ccl5 (RANTES) and Cxcl10 (IP-10; 25); thus, ATM may be related with radiation-induced fibrosis. Furthermore, it was reported that levels of Ccl5 (RANTES) and Cxcl10 (IP-10) in human acute myeloid leukemia cells from patients in the presence of fibroblasts were changed (26), and ataxia telangiectasia (A-T) patients sometimes caused leukemia (27). Thus, our findings in nonirradiated ATM-KO further suggest that these productions of chemokine in A-T patients may play a role for progressing leukemia.

Interestingly, another chemokine, Ccl3l3 (Mip-1α), which showed a very low expression in ATM-KO in both microarray analysis and ELISA, might also play an important role in cell migration under the condition of *Atm* deficiency. Furthermore, IPA done in this study

Published OnlineFirst February 25, 2011; DOI: 10.1158/1541-7786.MCR-10-0358

indicated that the expressions of 3 chemokine genes, that is, *Ccl2*, *Ccl3l3* (*Mip-1*α), and *Ccl4*, were decreased in ATM-KO, and these genes are reported to be regulated by fibrinogen (Fig. 1B; ref. 17, 18); thus, *Atm* deficiency may cause decrease in fibrinogen activity.

This study revealed for the first time that irradiated cells produce unknown soluble factors in the CM, and these factors can stimulate the expression of ISGs such as *Irf7* and *Stat1* in nnonirradiated neighbor cells, which may be a radiation-induced bystander effect.

Disclosure of Potential Conflicts of Interest

No potential conflicts of interest were disclosed.

Acknowledgments

The authors thank Mrs. Abe and Mr. M. Yoneya (Tohoku Environmental Sciences Services Corporation) for providing technical assistance in bleeding ATM-knockout mice. The microarray data presented in this article have been deposited in Gene Expression Omnibus (GEO; Accession no. GSE23116).

Grant Support

This work was supported by a contract with the Aomori Prefectural Government, Japan.

The costs of publication of this article were defrayed in part by the payment of page charges. This article must therefore be hereby marked *advertisement* in accordance with 18 U.S.C. Section 1734 solely to indicate this fact.

Received August 6, 2010; revised February 1, 2011; accepted February 18, 2011; published OnlineFirst February 25, 2011.

References

1. Banin S, Moyal L, Shieh S, Taya Y, Anderson CW, Chessa L, et al. Enhanced phosphorylation of p53 by ATM in response to DNA damage. Science 1998;281:1674–7.
2. Canman CE, Lim DS, Cimprich KA, Taya Y, Tamai K, Sakaguchi K, et al. Activation of the ATM kinase by ionizing radiation and phosphorylation of p53. Science 1998;281:1677–9.
3. Lee JH, Paull TT. Activation and regulation of ATM kinase activity in response to DNA double-strand breaks. Oncogene 2007;26:7741–8.
4. Lee JH, Paull TT. ATM activation by DNA double-strand breaks through the Mre11-Rad50-Nbs1 complex. Science 2005;308:551–4.
5. Haimovitz-Friedman A, Kan CC, Ehleiter D, Persaud RS, McLoughlin M, Fuks Z, et al. Ionizing radiation acts on cellular membranes to generate ceramide and initiate apoptosis. J Exp Med 1994;180:525–35.
6. Kolesnick R, Fuks Z. Radiation and ceramide-induced apoptosis. Oncogene 2003;22:5897–906.
7. Chen S, Wang G, Makrigiorgos GM, Price BD. Stable siRNA-mediated silencing of ATM alters the transcriptional profile of HeLa cells. Biochem Biophys Res Commun 2004;317:1037–44.
8. Mothersill C, Seymour C. Medium from irradiated human epithelial cells but not human fibroblasts reduces the clonogenic survival of unirradiated cells. Int J Radiat Biol 1997;71:421–7.
9. Matsumoto H, Takahashi A, Ohnishi T. Nitric oxide radicals choreograph a radioadaptive response. Cancer Res 2007;67:8574–9.
10. Matsumoto H, Takahashi A, Ohnishi T. Radiation-induced adaptive responses and bystander effects. Biol Sci Space 2004;18:247–54.
11. Yang H, Asaad N, Held KD. Medium-mediated intercellular communication is involved in bystander responses of X-ray-irradiated normal human fibroblasts. Oncogene 2005;24:2096–103.
12. Umesako S, Fujisawa K, Iiga S, Mori N, Takahashi M, Hong DP, et al. *Atm* heterozygous deficiency enhances development of mammary carcinomas in *p53* heterozygous knockout mice. Breast Cancer Res 2005;7:164–70.
13. Tsukada T, Tomooka Y, Takai S, Ueda Y, Nishikawa S, Yagi T, et al. Enhanced proliferative potential in culture of cells from p53-deficient mice. Oncogene 1993;8:3313–22.
14. Hickson I, Zhao Y, Richardson CJ, Green SJ, Martin NM, Orr AI, et al. Identification and characterization of a novel and specific inhibitor of the ataxia-telangiectasia mutated kinase ATM. Cancer Res 2004;64:9152–9.
15. Sugihara T, Magae J, Wadhwa R, Kaul SC, Kawakami Y, Matsumoto T, et al. Dose and dose-rate effects of low-dose ionizing radiation on activation of Trp53 in immortalized murine cells. Radiat Res 2004;162:296–307.
16. Sugihara T, Murano H, Tanaka K, Oghiso Y. Inverse dose-rate-effects on the expressions of extra-cellular matrix-related genes in low-dose-rate gamma-ray irradiated murine cells. J Radiat Res (Tokyo)2008;49:231–40.
17. Motojima M, Matsusaka T, Kon V, Ichikawa I. Fibrinogen that appears in Bowman's space of proteinuric kidneys *in vivo* activates podocyte Toll-like receptors 2 and 4 *in vitro*. Nephron Exp Nephrol 2010;114:e39–47.
18. Smiley ST, King JA, Hancock WW. Fibrinogen stimulates macrophage chemokine secretion through toll-like receptor 4. J Immunol 2001;167:2887–94.
19. Marié I, Durbin JE, Levy DE. Differential viral induction of distinct interferon-alpha genes by positive feedback through interferon regulatory factor-7. EMBO J 1998;17:6660–9.
20. David M, Petricoin E III, Benjamin C, Pine R, Weber MJ, Larner AC. Requirement for MAP kinase (ERK2) activity in interferon alpha- and interferon beta-stimulated gene expression through STAT proteins. Science 1995;269:1721–3.
21. Honda K, Yanai H, Negishi H, Asagiri M, Sato M, Mizutani T. IRF-7 is the master regulator of type-I interferon-dependent immune responses. Nature 2005;434:772–7.
22. Townsend PA, Cragg MS, Davidson SM, McCormick J, Barry S, Lawrence KM, et al. STAT-1 facilitates the ATM activated checkpoint pathway following DNA damage. J Cell Sci 2005;118:1629–39.
23. Takaoka A, Hayakawa S, Yanai H, Stoiber D, Negishi H, Kikuchi H, et al. Integration of interferon-alpha/beta signalling to p53 responses in tumour suppression and antiviral defence. Nature 2003;424:516–23.
24. Génin P, Algarté M, Roof P, Lin R, Hiscott J. Regulation of RANTES chemokine gene expression requires cooperativity between NF-kappa B and IFN-regulatory factor transcription factors. J Immunol 2000;164:5352–61.
25. Johnston CJ, Williams JP, Okunieff P, Finkelstein JN. Radiation-induced pulmonary fibrosis: examination of chemokine and chemokine receptor families. Radiat Res 2002;157:256–65.
26. Olsnes AM, Motorin D, Ryningen A, Zaritskey AY, Bruserud Ø. T lymphocyte chemotactic chemokines in acute myelogenous leukemia (AML): local release by native human AML blasts and systemic levels of CXCL10 (IP-10), CCL5 (RANTES) and CCL17 (TARC). Cancer Immunol Immunother 2006;55:830–40.
27. Stankovic T, Kidd AM, Sutcliffe A, McGuire GM, Robinson P, Weber P, et al. ATM mutations and phenotypes in ataxia-telangiectasia families in the British Isles: expression of mutant ATM and the risk of leukemia, lymphoma, and breast cancer. Am J Hum Genet 1998;62:334–45.

AACR American Association for Cancer Research

Molecular Cancer Research

Activation of Interferon-Stimulated Genes by γ-Ray Irradiation Independently of the Ataxia Telangiectasia Mutated–p53 Pathway

Takashi Sugihara, Hayato Murano, Masako Nakamura, et al.

Mol Cancer Res 2011;9:476-484. Published OnlineFirst February 25, 2011.